https://doi.org/10.15407/dopovidi2022.06.046
UDC 532.595

A.O. Milyaev[1]
A.N. Timokha[1,2], https://orcid.org/0000-0002-6750-4727
[1] Institute of Mathematics of the NAS of Ukraine, Kyiv
[2] Centre of Excellence "Autonomous Marine Operations and Systems",
Department of Marine Technology, Norwegian University of Science and Technology, Trondheim, Norway
E-mail: amilyaev@gmail.com, tim@imath.kiev.ua, atimokha@gmail.com

Learning the single-dominant modal system on resonant sloshing in a rectangular tank

Presented by Academician of the NAS of Ukraine A.N. Timokha

A machine learning technique is proposed to derive the damping rate functions in the co-called single-dominant modal system describing the resonant liquid sloshing in a rectangular tank performing harmonic longitudinal motions. Its implementation is demonstrated for the steady-state (periodic) resonance waves when the modal system admits an analytical asymptotic solution depending on the introduced damping rate functions. Recent experiments by Bäuerlein & Avila (2021) are employed to show that the viscous damping of the higher natural sloshing modes matters, and the damping functions depend on the wave amplitude.

Keywords: *sloshing, machine learning, damping.*

Two-dimensional nonlinear resonant sloshing in a rectangular tank is normally adopted as a benchmark problem for complex experimental-and-theoretical studies and developing & testing diverse Computational Fluid Dynamics (CFD) methods. The analytical studies assume an inviscid incompressible liquid with irrotational flows so that the viscous damping is neglected. A consequence of this simplification is that the phase lag between the steady-state (periodic) wave response and harmonic horizontal tank forcing becomes a *piecewise* function [1, chapter 8] possessing the values 0 and $\pm\pi$. Moreover, neglecting the viscous damping theoretically yields the *infinite* nonlinear resonant wave amplitude that has no a physical meaning.

Damping of the *linear* liquid sloshing is naturally associated with the laminar viscous boundary layer on the wetted tank surface. The related constant damping rates are theoretically & experimentally estimated & measured by Keulegan [2]. Chapter 6 in [1] discusses extra linear & *nonlinear* damping mechanisms incl. wave breaking and free-surface contamination. Extensive experimental studies are needed to judge on when and what from these mechanisms play a non-negligible role in theoretical analysis. Recent paper [3] represents an example of these experimental studies. Its authors measure the phase lag between the harmonic horizontal forcing and

Цитування: Milyaev A.O., Timokha A.N. Learning the single-dominant modal system on resonant sloshing in a rectangular tank. *Допов. Нац. акад. наук Укр.* 2022. № 6. С. 46—53.
https://doi.org/10.15407/dopovidi2022.06.046

steady-state (periodic) motions of the liquid mass centre. A reason for focusing on the phase lag is that the viscous damping causes a crucial effect on the phase lag converting it, as mentioned above, from piecewise to smooth function. The measurements used to estimate a suitable constant damping rate in the damped Duffing equation, which was *speculatively* adopted by the authors as a phenomenological model of the liquid mass centre motions. Such a constant damping rate was also employed in the lowest-order equation of the so-called single-dominant nonlinear modal system [4], which, as it was demonstrated in numerous publications (see, a review in [1]), satisfactory predicts the steady-state resonant sloshing when the forcing amplitude is relatively small, the forcing frequency is close to the lowest natural sloshing frequency, the liquid depth is not small, and the secondary resonance phenomenon [5] does not matter. The measurements in [3] show that the matched damping ratio $\xi = \text{const}$ in the Duffing mathematical model should be too far ($\xi = 15 \cdot 10^{-3}$) from predictions by Keulegan ($\xi = 5{,}7 \cdot 10^{-3}$) to fit the measured phase lag even for the lowest excitation amplitude when, no doubt, the single-dominant model system is applicable and the damping should mainly be associated with the viscous boundary layer effect [1, 5]. Adopting this larger damping rate in the lowest-order modal equation (damping of the higher natural sloshing modes is totally neglected by the authors) shows an insufficient consistency with the measured data which may wrongly conclude that either the single-dominant modal system is not applicable (no doubt, it is applicable) or the total energy dissipation is much larger than its estimate by Keulegan [2].

The single-dominant modal system [2, 4, 5] belongs to the co-called Reduced Order Models (ROMs) resulted from applying, simultaneously, projective, and asymptotic methods to the original free-surface "sloshing" problem. The present paper implements a machine learning algorithm [6] to restore the damping terms/functions in the modal system from a series of experimental data on the phase lag. Going this way, one is assumed that (i) damping of the higher natural sloshing modes *cannot* be neglected, (ii) the damping terms/functions depend on the wave amplitude [6], and (iii) the single-dominant modal system becomes inapplicable with increasing the forcing amplitude and, surely, it fails when experimental observations [3] report fragmentations of the free surfaces (e. g., due to the wave breaking). The factors (i-iii) are *fully ignored* in the theoretical manipulations [3] with the single-dominant modal system.

Let the horizontal tank dimension L be the characteristic size and $T = 2\pi/\sigma_1$ be the characteristic time (σ_1 is the lowest natural sloshing frequency). Then the "damped" non-dimensional single-dominant *nonlinear* asymptotic modal system [1, 4] for the horizontally-forced rectangular tank takes the following form

$$
\begin{aligned}
&\ddot{\beta}_1 + \beta_1 + 2\Xi_1(\beta_m, \dot{\beta}_m\,|_{m=1,\ldots,3})\dot{\beta}_1 + d_1(\ddot{\beta}_1\beta_2 + \dot{\beta}_1\dot{\beta}_2) + \\
&+ d_2(\ddot{\beta}_1\beta_1^2 + \dot{\beta}_1^2\beta_1) + d_3\ddot{\beta}_2\beta_1 = P_1\eta_{2a}\bar{\sigma}^2\cos(\bar{\sigma}t - \theta), \\
&\ddot{\beta}_2 + \bar{\sigma}_2^2\beta_2 + 2\bar{\sigma}_2\Xi_2(\beta_m, \dot{\beta}_m\,|_{m=1,\ldots,3})\dot{\beta}_2 + d_4\ddot{\beta}_1\beta_1 + d_5\dot{\beta}_1^2 = 0, \\
&\ddot{\beta}_3 + \bar{\sigma}_3^2\beta_3 + 2\bar{\sigma}_3\Xi_3(\beta_m, \dot{\beta}_m\,|_{m=1,\ldots,3})\dot{\beta}_3 + q_1\ddot{\beta}_1\beta_2 + q_2\ddot{\beta}_1\beta_1^2 + q_3\ddot{\beta}_2\beta_1 + \\
&+ q_4\dot{\beta}_1^2\beta_1 + q_5\dot{\beta}_1\dot{\beta}_2 = P_3\eta_{2a}\bar{\sigma}^2\cos(\bar{\sigma}t - \theta),
\end{aligned}
\tag{1}
$$

where the three hydrodynamic generalized coordinates $\beta_i(t)$, $i = 1, 2, 3$, come from the functional (Fourier) representation of the free surface

$$z = \zeta(y,t) = \sum_{i=1}^{\infty} \beta_1(t) \cos\left(\pi i\left(y + \frac{1}{2}\right)\right);$$

$$\beta_1 = O(\epsilon^{1/3}); \quad \beta_2 = O(\epsilon^{2/3}); \quad \beta_3 = O(\epsilon); \quad \beta_n = o(\epsilon), \quad n \geqslant 4; \quad \epsilon \ll 1, \tag{2}$$

σ_1 are the natural sloshing frequencies, $\bar{\sigma} = \sigma / \sigma_1$ (is the forcing frequency), $P_i = 2/(\pi i)\tanh(\pi i h)((-1)^i - 1)$, $\bar{\sigma}_m^2 = m\tanh(\pi m h)/\tanh(\pi h)$, the hydrodynamic coefficients d_n, q_n depend on the non-dimensional liquid depth h, η_{2a} is the non-dimensional forcing amplitude, and θ is the phase lag in the harmonic forcing. The computed values of the hydrodynamic coefficients are tabled in [1]. A novelty with respect to the original inviscid analysis in [1] consists of the generally non-constant damping terms $2\bar{\sigma}_i \Xi_i(\beta_m, \dot{\beta}_m|_{m=1,\ldots,3})\dot{\beta}_i$ incorporated into the modal system, where Ξ_i are *a priori* unknown *damping rate function*.

The steady-state resonant sloshing is associated with periodic solutions of (1). Following the Moiseev' asymptotic scheme which is described in [1, Chapter 8] derives the asymptotic periodic solution

$$\beta_1(t) = a\cos(\bar{\sigma}t) + a^3(k_1\cos(3\bar{\sigma}t) + k_2\sin(3\bar{\sigma}t)) + o(\epsilon),$$

$$\beta_2(t) = a^2(l_0 + l_1\cos(2\bar{\sigma}t) + l_2\sin(2\bar{\sigma}t)) + o(\epsilon), \tag{3}$$

$$\beta_3(t) = \epsilon[n_1\cos\bar{\sigma}t + n_2\sin\bar{\sigma}t] +$$
$$+ a^3[N_1\cos\bar{\sigma}t + N_2\sin\bar{\sigma}t + N_3\cos 3\bar{\sigma}t + N_3\sin 3\bar{\sigma}t] + o(\epsilon),$$

where $\epsilon = P_1\eta_{2a} \ll 1$, $a = O(\epsilon^{1/3})$ is the dominant wave amplitude, and

$$l_0 = \frac{d_4 - d_5}{2\bar{\sigma}_2^2},$$

$$l_1(a) = \frac{(d_4 + d_5)(\bar{\sigma}_2^2 - 4)}{2((\bar{\sigma}_2^2 - 4)^2 + 16\bar{\sigma}_2^2\Xi_2^2(a))},$$

$$l_2(a) = \frac{2(d_4 + d_5)\bar{\sigma}_2\Xi_2(a)}{((\bar{\sigma}_2^2 - 4)^2 + 16\bar{\sigma}_2^2\Xi_2^2(a))};$$

$$k_1(a) = \frac{\frac{1}{2}d_2(\bar{\sigma}_1^2 - 9) + (\frac{3}{2}d_1 + 2d_3)(l_1(\bar{\sigma}_1^2 - 9) - 6\bar{\sigma}_1\Xi_1(a)l_2)}{(\bar{\sigma}_1^2 - 9)^2 + 36\bar{\sigma}_1^2\Xi_1^2(a)},$$

$$k_2(a) = \frac{3d_2\bar{\sigma}_1\Xi_1(a) + (\frac{3}{2}d_1 + 2d_3)(l_2(\bar{\sigma}_1^2 - 9) + 6\bar{\sigma}_1\Xi_1(a)l_1)}{(\bar{\sigma}_1^2 - 9)^2 + 36\bar{\sigma}_1^2\Xi_1^2(a)};$$

$$n_1(a) = \frac{P_3(\cos\theta(\bar{\sigma}_3^2 - 1) - 2\sigma_3\Xi_3(a)\sin\theta)}{P_1((\bar{\sigma}_3^2 - 1)^2 + 4\bar{\sigma}_3^2\Xi_3^2(a))},$$

$$n_2(a)=\frac{P_3(2\sigma_3\Xi_3(a)\cos\theta+(\overline{\sigma}_3^2-1)\sin\theta)}{P_1((\overline{\sigma}_3^2-1)^2+4\overline{\sigma}_3^2\Xi_3^2(a))};$$

$$N_1(a)=\frac{(l_1(\overline{\sigma}_3^2-1)-2\overline{\sigma}_3\Xi_3(a)l_2)(\frac{1}{2}q_1+2q_3-q_5)+(\frac{3}{4}q_2-\frac{1}{4}q_1+q_1l_0)(\overline{\sigma}_3^2-1)}{(\overline{\sigma}_3^2-1)^2+4\overline{\sigma}_3^2\Xi_3^2(a)},$$

$$N_2(a)=\frac{(l_2(\overline{\sigma}_3^2-1)+2\overline{\sigma}_3\Xi_3(a)l_1)(\frac{1}{2}q_1+2q_3-q_5)+2\Xi_3\overline{\sigma}_3(\frac{3}{4}q_2-\frac{1}{4}q_1+q_1l_0)}{(\overline{\sigma}_3^2-1)^2+4\overline{\sigma}_3^2\Xi_3^2(a)},$$

$$N_3(a)=\frac{(l_1(\overline{\sigma}_3^2-9)-6\overline{\sigma}_3\Xi_3(a)l_2)(\frac{1}{2}q_1+2q_3+q_5)+\frac{1}{4}(q_2+q_4)(\overline{\sigma}_3^2-9)}{(\overline{\sigma}_3^2-9)^2+36\overline{\sigma}_3^2\Xi_3^2(a)},$$

$$N_4(a)=\frac{(l_2(\overline{\sigma}_3^2-9)+6\overline{\sigma}_3\Xi_3(a)l_1)(\frac{1}{2}q_1+2q_3+q_5)+3(q_2+q_4)\overline{\sigma}_3\Xi_3(a)}{(\overline{\sigma}_3^2-9)^2+36\overline{\sigma}_3^2\Xi_3^2(a)}$$

are functions of $a=O(\epsilon^{1/3})>0$ and, generally, θ when it comes to $\beta_3(t)$. Because the lowest-order term in (3) is associated with $\beta_1(t)=a\cos(\overline{\sigma}t)$, which is purely cosine function, θ *is, in fact, the phase lag between the forcing and the wave response in the lowest-order asymptotic approximation.*

According to the standard Moiseev's asymptotic procedure [1], the unknown amplitude parameter a and phase lag θ can be found from the so-called *secular system*

$$(m_1a^2+(\hat{\sigma}^2-1))a=\epsilon\cos\theta,\quad (m_2a^2-2\Xi_1(a))a=\epsilon\sin\theta, \tag{4}$$

in which

$$m_1=m_1(\Xi_1(a),\Xi_2(a))=-\frac{1}{2}d_2-2d_3l_1+d_1\left(-l_0+\frac{1}{2}l_1\right),$$

$$m_2=m_2(\Xi_1(a),\Xi_2(a))=\frac{1}{2}l_2(d_1-4d_3);$$

$$\epsilon=P_1\eta_{2a};\quad \hat{\sigma}=\overline{\sigma}^{-1}.$$

Taking the sum of squares in (4) makes it possible to rewrite the secular system to the two equations,

$$a^2[(m_1(\Xi_1(a),\Xi_2(a))a^2+(\hat{\sigma}^2-1))^2+(m_2(\Xi_1(a),\Xi_2(a))a^2-2\Xi_1(a))^2]=\epsilon^2 \tag{5}$$

and

$$\theta=\operatorname{atan2}(\epsilon^{-1}[m_2(\Xi_1(a),\Xi_2(a))a^2-2\Xi_1(a)],\epsilon^{-1}[m_1(\Xi_1(a),\Xi_2(a))a^2+(\hat{\sigma}^2-1)]). \tag{6}$$

Consequently solving (5) and (6) outputs the dominant wave amplitude parameter $a>0$ and the phase lag θ as a function of $\hat{\sigma}$. The procedure assumes that $\Xi_m(a)$, $m=1,2$, are known functions of a. *This is not true in our case.*

In the forthcoming analysis, we suppose that there exist experimental measurements of the phase lag versus the forcing frequency, i. e. $((\overline{\sigma})_i, \theta_i)\,|_{\eta_{2a}}$, $i = 1, \ldots, N_{\eta_{2a}}$ for the fixed non-dimensional liquid depth h and several forcing amplitudes η_{2a}. A *machine learning technique* can then be utilised to get an approximation of $\Xi_m(a)$ using these measurements. Because $a = O(\epsilon^{1/3})$ is the small parameter, an adequate approximation of $\Xi_1(a)$ and $\Xi_2(a)$ takes the polynomial form

$$\Xi_1(a;\{x_m\}) = \sum_{\{m=0\}}^{N} x_m a^m, \quad \Xi_2(a;\{x_m\}) = \sum_{\{m=0\}}^{N-1} y_m a^m, \tag{7}$$

where we accounted for that $\beta_2 = \beta_1 O(\epsilon^{1/3}) \Rightarrow \Xi_2 = \Xi_1 O(\epsilon^{1/3})$.

Substituting (7) into (5) and extracting the forcing frequency gives

$$\hat{\sigma}^2(a;\{x_m\},\{y_m\};\eta_{2a}) = 1 - m_1(a;\{y_m\})a^2 \pm \sqrt{\frac{\epsilon^2}{a^2} - (m_2(a;\{y_m\})a^2 - 2\Xi_1(a;\{x_m\}))^2},$$

which has a physical meaning when both the right-hand side and expression under the square root are non-negative. The existence conditions yield the interval $a_{\min}(\eta_{2a},\{x_m\},\{y_m\}) \leqslant a \leqslant a_{\max}(\eta_{2a},\{x_m\},\{y_m\})$ depending on $\{x_m\},\{y_m\}$ and η_{2a}. Changing a in the interval outputs $\hat{\sigma}^2(a;\{x_m\},\{y_m\};\eta_{2a})$ as a function of the lowest-order amplitude parameter for the fixed values of $\{x_m\},\{y_m\}$ and η_{2a}. Inserting $\hat{\sigma}^2(a;\{x_m\},\{y_m\};\eta_{2a})$ into (6) derives

$$\theta(a;\{x_m\},\{y_m\};\eta_{2a}) = \operatorname{atan2}[m_2(a;\{y_m\})a^2 - 2\Xi_1(a;\{x_m\}), m_1(a;\{y_m\})a^2 +$$

$$+(\hat{\sigma}^2(a;\{x_m\},\{y_m\};\eta_{2a}) - 1)] \tag{8}$$

as a function of a on the interval $a_{\min}(\eta_{2a},\{x_m\},\{y_m\}) \leqslant a \leqslant a_{\max}(\eta_{2a},\{x_m\},\{y_m\})$ for the fixed $\{x_m\},\{y_m\}$ and η_{2a}.

Using the exact solution (8) and the machine learning makes it possible to compute $\{x_m\},\{y_m\}$. For this purpose, we introduce the distance function $D(\eta_{2a}, i;\{x_m\},\{y_m\})$ between the theoretical phase-lag curve by (8) with the fixed $\{x_m\},\{y_m\}$; η_{2a}, and a fixed experimental point $((\overline{\sigma})_i, \theta_i)\,|_{\eta_{2a}}$:

$$D^2(\eta_{2a}, i;\{x_m\},\{y_m\}) = \min_{a_{\min}(\eta_{2a},\{x_m\},\{y_m\}) \leqslant a \leqslant a_{\max}(\eta_{2a},\{x_m\},\{y_m\})} [(\overline{\sigma}(a;\{x_m\},\{y_m\};\eta_{2a}) - (\overline{\sigma})_i^{\eta_{2a}})^2 +$$

$$+(\theta(a;\{x_m\},\{y_m\};\eta_{2a}) - \theta_i^{\eta_{2a}})^2].$$

Utilising the distance function determines the loss function

$$C(\{x_m\},\{y_m\}) = \sum_{\eta_{2a}} \sum_{i=1}^{N_{\eta_{2a}}} D(\eta_{2a}, i;\{x_m\},\{y_m\}), \tag{9}$$

which characterises the summarised distance between the measured values $((\overline{\sigma})_i, \theta_i)\,|_{\eta_{2a}}$, $i = 1, \ldots, N_{\eta_{2a}}$ and the theoretical curve by (8). Minimisation of the loss function (9) can be done by using the gradient descent.

Example. The experimental data on the liquid mass centre (amplitude and phase lag) were reported in [3] for the non-dimensional depth $h = 0.8$, which implies [1] $d_1 = 3.142$, $d_2 = 2.533$,

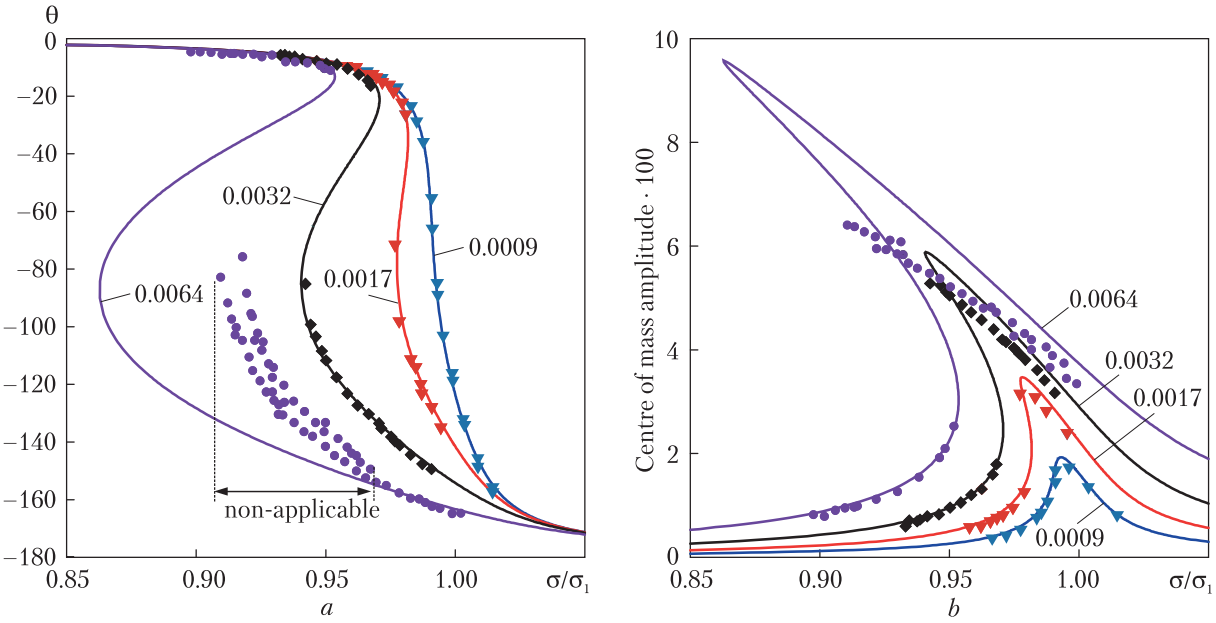

The phase lag (*a*) and the maximum deviation of the liquid mass centre (*b*) for the steady-state sloshing in a rectangular tank with input parameters from the experimental paper [3]. The single-dominant nonlinear modal system with the damping rate functions (1) is used to derive the steady-state wave solution (3). The measured phase lag with the lowest forcing amplitudes $\eta_{2a} = 0.0009, 0.0017,$ and 0.0032 are used to learn by the linear regression for Ξ_1 and the constant approximation of Ξ_2 by the measured phase lag in the panel *a*. The experimental data for the largest forcing amplitude $\eta_{2a} = 0.0064$ (when the single-dominant modal system is, generally, inapplicable) are used in *a* to test the learnt damping rate functions. The panel *b* also tests the learnt damping rate functions by comparing the theory and the measured maximum steady-state displacement of the liquid mass centre in the horizontal direction

$d_3 = -0.021$, $d_4 = -0.042$, $d_5 = -3.225$. The measurements were done for the forcing non-dimensional amplitudes equal to $\eta_{2a} = 0.0009,\ 0.0017,\ 0.0032$, and 0.0064. The liquid mass centre non-dimensional motions in the horizontal direction are theoretically described by the formula [1, Eq. (8.73)]

$$y_C(t) = -\frac{2}{\pi^2 h}(\beta_1(t) + \frac{1}{9}\beta_3(t)) + o(\epsilon) =$$

$$= -\frac{2}{\pi^2 h}([a + \frac{1}{9}(a^3 N_1 + \epsilon n_1)]\cos\bar{\sigma}t + \frac{1}{9}[a^3 N_2 + \epsilon n_2]\sin\bar{\sigma}t +$$

$$+ a^3[(k_1 + \frac{1}{9}N_3)\cos 3\bar{\sigma}t + (k_2 + \frac{1}{9}N_4)\sin 3\bar{\sigma}t]) + o(\epsilon). \qquad (10)$$

Let us demonstrate the learning technique by assuming the linear regression for the first damping rate function, i. e., $\Xi_1(a; x_0, x_1) = x_0 + x_1 a$ and the constant damping rate for the second natural sloshing mode (generalised coordinate), $\Xi_2(a; y_0) = y_0$, where the constant values x_0 and y_0 correspond to the damping rates for the first and second natural sloshing modes whose asymptotic estimate (from below) was given by Keulegan [2]. Using three measurement series with $\eta_{2a} = 0.0009, 0.0017,$ and 0.0032 from [3] computes $x_0 = 0.00717$, $x_1 = 0.00189$, and $y_0 = 0.01$.

The fourth experimental series with $\eta_{2a} = 0.0064$ was characterised by amplification of higher harmonics and the wave breaking phenomenon on the free surface that indicates inapplicability of the single-dominant modal system.

The first test for the learnt x_0 and y_0 consists of comparison with predictions by Keulegan [3]. According to the Keulegan's estimate of the laminar viscous boundary layer effect, the viscous damping rates should be $x_0 = 0.0057$ and $y_0 = 0.008$, respectively. Because Keulegan's formula gives the estimate from below, this is rather good agreement with the computed values $x_0 = 0.00717$ and $y_0 = 0.01$ by the machine learning algorithm. The experimental tank breadth was rather small (0.05 m) and, therefore, the dynamic contact angle effect on the damping rates cannot be neglected. Why the dynamic contact angle gives a contribution to the damping rates in narrow tanks was discussed in [3] and [1, chapter 6]. On the other hand, Bäuerlein & Avila [3] concluded that the damping rate x_0 should be much larger, equal to 0.015 to fit the experimental measurements with the Duffing mathematical model. Their error is caused by neglecting the second natural sloshing mode effect and its damping as well as they ignored the dependence on a in Ξ_1.

Theoretical and experimental values of the phase lag and the maximum deviations of the mass centre by (10) are compared in the panels *a* and *b* of Figure, respectively. As we mentioned above, three experimental series in *a* were used to learn the damping functions but the experimental case with $\eta_{2a} = 0.0064$ was adopted for testing the results. For the learning amplitudes $\eta_{2a} = 0.0009, 0.0017,$ and 0.0032 in Figure, *a*, incorporating the computed damping functions made it possible to perfectly fit the experimental points. Figure, *a* with $\eta_{2a} = 0.0064$ shows that the theoretical results for the phase lag are not consistent with experiments in the frequency domain where the single-dominant modal system (1) is not applicable (in this frequency domain, [3] reports amplification of higher harmonics and surface wave phenomena alike the wave breaking). Far from this zone, the damping rate functions are well-predicted and the single-dominant nonlinear modal system is no doubt applicable.

Figure, *b* tests the learnt damping function by the measured maximum deviations of the liquid mass centre, which can theoretically be computed by (10). A discrepancy is obviously observed for the largest forcing amplitude when, as we mentioned above, the single-dominant modal system is not applicable whilst the case with the lowest forcing amplitude shows an almost perfect agreement with the learnt damping functions. The discrepancy for $\eta_{2a} = 0.0017$ and 0.0032 is only serious in the vicinity of the maximum amplitude response and it looks like in [8] where analogous discrepancy was explained by amplification of the higher generalised coordinates that requires an adaptive multimodal modelling.

Conclusions. An accurate implementation of the single-dominant nonlinear modal system with the learnt damping terms shows that conclusion in [3] that the actual damping is much larger than Keulegan's estimate by the laminar viscous boundary layer effect is generally wrong. To account correctly for the viscous damping in the modal system, one must introduce the damping functions in the higher order modal equations and these damping functions should depend on the wave amplitude.

The second author acknowledges the financial support of the National Research Foundation of Ukraine (Project number 2020.02/0089) and a partial support of Centre of Autonomous Marine Operations & Systems (AMOS) whose main sponsor is the Norwegian Research Council (Project number 223254-AMOS).

REFERENCES

1. Faltinsen, O. M. & Timokha, A. N. (2009). Sloshing. Cambridge University Press.
2. Keulegan, G. H. (1959). Energy dissipation in standing waves in rectangular basins. J. Fluid Mech., 6, pp. 33-50. https://doi.org/10.1017/S0022112059000489
3. Bäuerlein, B. & Avila, K. (2021). Phase lag predicts nonlinear response maxima in liquid-sloshing experiments. J. Fluid Mech., 925, A22, pp. 1-29. https://doi.org/10.1017/jfm.2021.576
4. Hermann, M. & Timokha, A. (2005). Modal modelling of the nonlinear sloshing in a circular tank I: A single-dominant model. Math. Models Methods Appl. Sci., 15, No 9, pp. 1431-1458. https://doi.org/10.1142/S0218202505000777
5. Hermann, M. & Timokha, A. (2008). Modal modelling of the nonlinear sloshing in a circular tank II: Secondary resonance. Math. Models Methods Appl. Sci., 18, No 11, pp. 1845-1867. https://doi.org/10.1142/S0218202508003212
6. Ahmed, S. E., Pawar, S., San, O., Rasheed, A., Iliescu, T. & Noack, B. R. (2021). On closures for reduced order models — A spectrum of first-principle to machine-learned avenues. Phys. Fluids, 33, Art. 091301, 32 p. https://doi.org/10.1063/5.0061577
7. Raynovskyy, I. A. & Timokha, A. N. (2018). Damped steady-state resonant sloshing in a circular container. Fluid Dyn. Res., 50, Art. 045502, 20 p. https://doi.org/10.1088/1873-7005/aabe0e
8. Faltinsen, O. M. & Timokha, A. N. (2001). Adaptive multimodal approach to nonlinear sloshing in a rectangular tank. J. Fluid Mech., 432, pp. 167-200. https://doi.org/10.1017/S0022112000003311

Received 14.06.2022

А.О. Міляєв[1]
О.М. Тимоха[1,2], https://orcid.org/0000-0002-6750-4727

[1] Інститут математики НАН України, Київ

[2] Центр досконалості “Автономні морські операції та системи”,
Департамент Морських технологій, Норвезький університет природничих та технічних наук,
Трондхейм, Норвегія

E-mail: amilyaev@gmail.com, tim@imath.kiev.ua, atimokha@gmail.com

НАВЧАННЯ МОДАЛЬНОЇ СИСТЕМИ З ОДНІЄЮ ДОМІНАНТНОЮ УЗАГАЛЬНЕНОЮ ГІДРОДИНАМІЧНОЮ КООРДИНАТОЮ, ЩО ОПИСУЄ РЕЗОНАНСНІ КОЛИВАННЯ РІДИНИ В ПРЯМОКУТНОМУ РЕЗЕРВУАРІ

Запропоновано техніку машинного навчання для отримання функції демпфування у так званій однодомінантній модальній системі, яка описує резонансне хлюпання рідини в прямокутному резервуарі, що перебуває у стані гармонічного поздовжнього збурення. Її реалізація продемонстрована для усталених (періодичних) хвиль, коли модальна система допускає аналітичний асимптотичний розв’язок, який залежить від введених функцій демпфування. Нещодавні експерименти Bäuerlein & Avila (2021) використовуються для того, аби показати, що демпфування вищих власних форм коливання рідини має значення і в’язке демпфування є функцією амплітуди хвилі.

Ключові слова: *хлюпання рідини, машинне навчання, демпфування.*